Available online at www.sciencedirect.com
ScienceDirect
Journal of Hazardous Materials 143 (2007) 396–408
Journal of Hazardous Materials
www.elsevier.com/locate/jhazmat

Kinetics and equilibrium modelling of lead uptake by algae *Gelidium* and algal waste from agar extraction industry

Vítor J.P. Vilar, Cidália M.S. Botelho, Rui A.R. Boaventura *

Laboratory of Separation and Reaction Engineering (LSRE), Departamento de Engenharia Química, Faculdade de Engenharia da Universidade do Porto, Rua Dr. Roberto Frias, 4200-465 Porto, Portugal

Received 19 June 2006; received in revised form 14 September 2006; accepted 15 September 2006
Available online 20 September 2006

Abstract

Pb(II) biosorption onto algae *Gelidium*, algal waste from agar extraction industry and a composite material was studied. Discrete and continuous site distribution models were used to describe the biosorption equilibrium at different pH (5.3, 4 and 3), considering competition among Pb(II) ions and protons. The affinity distribution function of Pb(II) on the active sites was calculated by the Sips distribution. The Langmuir equilibrium constant was compared with the apparent affinity calculated by the discrete model, showing higher affinity for lead ions at higher pH values.

Kinetic experiments were conducted at initial Pb(II) concentrations of 29–104 mg l^{-1} and data fitted to pseudo-first Lagergren and second-order models.

The adsorptive behaviour of biosorbent particles was modelled using a batch mass transfer kinetic model, which successfully predicts Pb(II) concentration profiles at different initial lead concentration and pH, and provides significant insights on the biosorbents performance. Average values of homogeneous diffusivity, D_h, are 3.6×10^{-8}; 6.1×10^{-8} and 2.4×10^{-8} cm^2 s^{-1}, respectively, for *Gelidium*, algal waste and composite material. The concentration of lead inside biosorbent particles follows a parabolic profile that becomes linear near equilibrium.

Keywords: Biosorption; Equilibrium; Kinetics; Algae *Gelidium*; Algal waste

1. Introduction

Although many countries have initiated programmes to lower the level of lead in the environment, human exposure to lead remains a concern to public health officials worldwide. Lead and its compounds may enter the environment during mining, smelting, processing, use, recycling or disposal. Major uses are in batteries, cables, pigments, gasoline additives, solder and steel products. Lead and lead compounds are also used in solder applied to water distribution pipes and to seams of cans used to store foods, in some traditional remedies, in bottle closures for alcoholic beverages and in ceramic glazes and crystal tableware [1].

In humans, lead can result in a wide range of biological effects depending upon the level and duration of exposure. Effects at the sub cellular level, as well as effects on the overall functioning of the body, have been noted and range from inhibition of enzymes to the production of marked morphological changes and death. The effects of lead on the haemopoietic system result in decreased haemoglobin synthesis [1].

Increasingly strict discharge limits on lead have accelerated the search for highly efficient and economically attractive treatment methods. Biosorption is an emerging recent technology, with effectiveness in reducing the concentration of metal ions to very low levels and the use of inexpensive biosorbent materials.

Removal of lead by sorption processes has been studied by several workers, using tree fern [2], soil bacterium [3], waste brewery biomass [4], peat moss [5] and different kinds of marine biomass [6–8] as biosorbents.

In this work, biosorption of lead ions has been studied assuming that it takes place by complexation with functional groups, by adsorption and ion exchange [9]. The characterization of algae *Gelidium*, algal waste and composite material binding sites (the biosorbents used in this work) was performed by potentiometric titrations [10]. Obtained results show a heterogeneous distribution of two binding sites, carboxylic and hydroxyl groups. Biosorption of copper by those materials was

* Corresponding author. Tel.: +351 225081683; fax: +351 225081674.
E-mail address: bventura@fe.up.pt (R.A.R. Boaventura).

0304-3894/$ – see front matter © 2006 Elsevier B.V. All rights reserved.
doi:10.1016/j.jhazmat.2006.09.046

well described by discrete and continuous distribution model, including competition between copper ions and protons for the binding sites [10]. At low pH values, carboxyl groups are protonated and thereby become less available for binding of metals, which explains why the binding of many metals increases with increasing pH.

The uptake of lead ions decreases by increasing the solution ionic strength. For high ionic strengths, adsorption sites will be surrounded by counter ions and they partially lose their charge, which weakens electrostatic interactions. Increasing temperature from 10 to 35 °C, increases slightly lead biosorption by algal waste and *Gelidium*, suggesting that the process is endothermic [11].

Kinetic studies of lead biosorption by algae *Gelidium*, algal waste and composite material were performed at different initial lead concentration and pH, and results were fitted by two mass transfer models. Equilibrium was studied at different pH values and the obtained results adjusted to discrete and continuous models.

2. Materials and methods

2.1. Biosorbents

Algal waste from agar extraction industry and the same waste granulated with polyacrylonitrile were used in this study as biosorbents, as well as algae *Gelidium*, the raw material for agar extraction. The characteristics and preparation of all these materials have been described in previous works [12,13].

2.2. Lead solutions

Pb(II) solutions were prepared by dissolving a weighted quantity of anhydrous $PbCl_2$ (Merck-Schuchardt, purity >98%) in distilled water. The pH was controlled at 3, 4 and 5.3 by the addition of 0.01 M HCl and NaOH solutions.

2.3. Kinetic studies

In order to determine the contact time required to reach equilibrium, batch biosorption dynamic experiments were performed at an initial Pb(II) concentration around 100 mg l^{-1}. pH and temperature were monitored and controlled throughout each experiment (pH/temperature meter WTW 538). In a typical batch biosorption kinetic experiment the vessel was filled with 0.5 l of distilled water, a known weight of biomass (2 g—algae *Gelidium* and algal waste; 1 g—composite material) was added and the suspension was stirred for 20 min (magnetic stirrer Heidolph MR 3000 operating at 600 rpm). Then, the metal solution (200 mg l^{-1}) was added and the suspension maintained at constant pH (5.3, 4 or 3) and temperature ($T = 20$ °C). Samples were taken after the addition of metal solution at pre-determined time intervals, ranging from 1 to 10 min until equilibrium was reached. They were centrifuged (Eppendorf Centrifuge 5410) and the supernatant analysed for Pb(II).

2.4. Equilibrium studies

The experiments were conducted in duplicate, using 100 ml Erlenmeyer flasks, at constant pH (5.3, 4 or 3) and temperature ($T = 20$ °C). The initial metal concentration varied between 10 and 300 mg Pb l^{-1}. A known weight of material (0.2 g—algae *Gelidium* and algal waste; 0.1 g—composite material) was suspended in 50 ml of distilled water and stirred at 100 rpm for 10 min; 50 ml of metal solution was added to the suspension; correction of pH was achieved by addition of NaOH and HCl diluted solutions and temperature was maintained constant using a HOTTECOLD thermostatic refrigerator; once equilibrium was reached, 1 h later, samples were taken and centrifuged (Eppendorf Centrifuge 5410) and the supernatant was analysed for the remaining Pb(II).

2.5. Analytical procedure

Pb(II) concentrations in the supernatants were determined by atomic absorption spectrometry (GBC 932 Plus Atomic Absorption Spectrometer), with deuterium background correction and a spectral slit width of 1.0 nm. The working current/wavelength was adjusted to 5.0 mA/217.0 nm, giving a detection limit of 1 ppm. The instrument response was periodically checked with Pb^{2+} solution standards.

The amount of metal adsorbed per gram of biosorbent was calculated as follows:

$$q = \frac{V(C_i - C_f)}{W} \quad (1)$$

where q is the metal uptake (mg metal g^{-1} of the biosorbent); C_i and C_f the initial and final metal concentrations in solution (mg l^{-1}); V the volume of solution (l); W is the dry weight of the added biosorbent (g).

3. Modelling lead biosorption

3.1. Discrete equilibrium model

The discrete model assumes that the biosorbent cell walls have one kind of predominant active sites (carboxylic groups), which are responsible for metal biosorption at pH < 7.0, and competition between metal ions and protons exists. The model defines two apparent equilibrium-binding constants, K_H and K_M, for protons and divalent metal cations, respectively, sorbing onto biomass binding sites according to the following equation:

$$q_M = \frac{Q_{max} K_M C_M}{1 + K_H C_H + K_M C_M} \quad (2)$$

where q_M is the equilibrium uptake capacity of the metal (mmol g^{-1}); Q_{max} the concentration of carboxylic groups (mmol g^{-1}); C_M and C_H are the equilibrium metal and proton concentrations in solution (mmol l^{-1}).

3.2. Continuous equilibrium model

For heterogeneous active sites, with a continuous distribution of affinities given by Sips distribution, assuming competition between metal ions and protons, and lead biosorption only on carboxylic groups (pH < 7.0), the continuous model is defined as

$$q_M = Q_{max}\frac{n_M}{n_H}\frac{(K'_M C_M)^{n_M}\{(K'_H C_H)^{n_H} + (K'_M C_M)^{n_M}\}^{p-1}}{1 + \{(K'_H C_H)^{n_H} + (K'_M C_M)^{n_M}\}^{p}} \quad (3)$$

where K'_H and K'_M are average values of the affinity constant distribution for proton and metal; p the generic or intrinsic heterogeneity of the biosorbent (is the generic width of the Sips distribution) and is common to all components; n_M and n_H accounts for the ion specific heterogeneity or non-ideality, which can be due to lateral interactions and/or stoichiometric effects ($n_X \neq 1$ non-ideal, $n_X = 1$ ideal). Data for metal ion binding are necessary in order to split the apparent heterogeneity ($m_X = n_X p$) into a generic or intrinsic heterogeneity part seen by all ions (p) and an ion-specific non-ideality part seen by each particular ion (n_X).

3.3. Kinetics

Kinetic models are used to examine the controlling mechanism of the biosorption process, mass transfer or chemical reaction. The two sorption kinetic models used in this study are based on the Ritchie equation. From the general form of the Ritchie equation, the pseudo-first-order Lagergren model and second-order kinetics can be deduced [13]:

$$\text{First-order Lagergren model}: \quad q_t = q_M[1 - \exp(-k_{1,ads}t)] \quad (4)$$

$$\text{Second-order model}: \quad q_t = \frac{q_M^2 k_{2,ads} t}{1 + k_{2,ads} q_M t} \quad (5)$$

where q_t is the concentration of ionic species in the sorbent at time t (mg metal g^{-1} biosorbent); $k_{1,ads}$ the biosorption constant of pseudo-first-order Lagergren equation (min^{-1}); $k_{2,ads}$ is the biosorption constant of pseudo-second-order equation (min^{-1} g biosorbent mg^{-1} metal).

The initial biosorption rate ($r_{ads}(i)$) can be calculated from

$$\left.\frac{dq}{dt}\right|_{t=0} = r_{ads}(i) \quad (6)$$

So,

$$r_{ads}(i) = k_{1,ads} q_M \quad (7)$$

and

$$r_{ads}(i) = k_{2,ads} q_M^2 \quad (8)$$

for the pseudo-first-order Lagergren (Eq. (7)) and pseudo-second-order models (Eq. (8)), respectively.

3.4. Mass transfer models

Algae *Gelidium* and algal waste biomass particles are uni-dimensional thin plates, with a width and length that greatly exceeds the thickness. Therefore, diffusion parallel to the normal of the surface corresponds to the shortest diffusion distance and determines the overall diffusion rate.

In a previous work [12], it has been concluded that particle size has no influence in the biosorption of lead ions by the spherical composite material, when comparing the range 0.5–1.0 and 1.0–1.4 mm diameter. This result is not in accordance with the general notion that the particle diffusion controls the overall sorption process. As the algal particles in the composite material are like thin plates, with the same thickness for all size fractions, the obtained result suggests that these particles are the active component in the sorption process, which determines the diffusion rate.

For a quantitative description of biosorption process dynamics, the following assumptions have been made:

1. negligible external film diffusion, for an adequate stirring rate;
2. sorption rate controlled by homogeneous diffusion inside the particle or linear driving force model (LDF);
3. isothermal process;
4. equilibrium between bounded and soluble metal concentrations, as formulated by Langmuir isotherms;
5. particles like uni-dimensional thin plates.

To demonstrate that concentration profiles inside the particle can be predicted either by the homogeneous diffusion model or the linear driving force model (the last one can be analytically solved), these two models have been developed.

3.4.1. Homogeneous diffusion model

Mass conservation inside the particles:

$$\frac{\partial y(x,t)}{\partial t} = \frac{1}{\tau_d}\frac{\partial^2 y(x,t)}{\partial x^2} \quad (9)$$

$$\tau_d = \frac{L^2}{D_h} \quad \text{(time constant for diffusion of ionic species into the particle, min)} \quad (10)$$

where D_h is the coefficient of homogeneous diffusion inside the particle ($cm^2\ s^{-1}$), L is half of the thin plate thickness (cm).

The initial and boundary conditions for Eq. (9) are:

$$t = 0: \quad y_b(0) = 1; \qquad 0 \le x \le 1: \quad y(x,0) = 0;$$
$$x = 1: \quad y(1,0) = \frac{K_L C_{b_0}}{1 + K_L C_{b_0}} \quad (11)$$

$$x = 0: \quad \frac{\partial y(x,t)}{\partial t} = 0, \quad \forall t \quad (12)$$

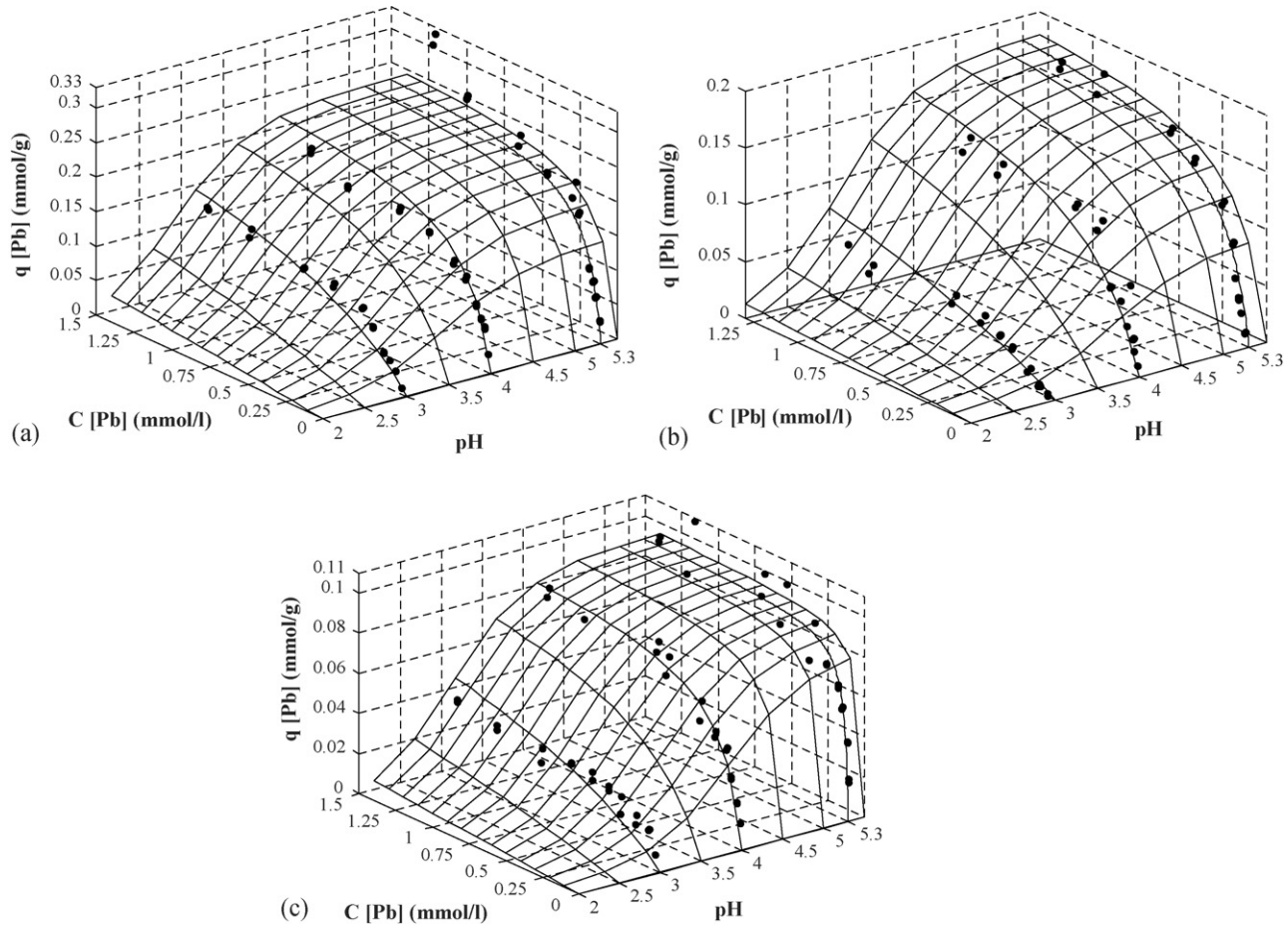

Fig. 1. Lead sorption isotherm surface: experimental data and discrete equilibrium model mesh. Solution pH 3, 4 and 5.3, lead concentration 0.0–1.5 mmol l^{-1}. Algae *Gelidium* (a), algal waste (b) and composite material (c).

$$x = 1: \quad \frac{\partial y(x,t)}{\partial t} = -\frac{\xi}{\tau_d} K_L C_{b_0} [1 - y(x,t)]^2 \left[\frac{\partial y(x,t)}{\partial x}\right]_{x=1}, \quad \forall t \tag{13}$$

Dimensionless variables:

$$y_b(t) = \frac{C_b(t)}{C_{b_0}}; \qquad y(x,t) = \frac{q(z,t)}{q_{max}}; \qquad \langle y(x,t)\rangle = \frac{\langle q(z,t)\rangle}{q_{max}};$$

$$x = \frac{z}{L}; \qquad y_M = \frac{q_M}{q_{max}}; \qquad \xi = \frac{W q_{max}}{V C_{b_0}}$$

where V is the metal solution volume (l); W the mass of biosorbent (g); $C_b(t)$ and $\langle q(z,\ t)\rangle$, respectively, the concentration of metal species in the liquid phase (mg l^{-1}) and the average metal concentration in the solid phase (mg g^{-1}); z the distance (expressed in cm) to the symmetry plane, C_{b_0} the initial metal concentration in the liquid phase (mg l^{-1}); $y_b(t)$ and $y(x,\ t)$ the dimensionless metal concentrations in liquid and solid phase; $\langle y(x,\ t)\rangle$ the dimensionless average metal concentration in the solid phase; x the dimensionless axial coordinate inside the particle; y_M the dimensionless metal concentration in the solid phase, given by the equilibrium law; ζ is the dimensionless factor for the batch capacity.

Predicting metal ion concentration requires the knowledge of six parameters: equilibrium isotherm parameters (q_{max}, K_L) at the solution pH, solution volume (V), initial Pb(II) concentration (C_{b_0}), biomass particles load (W) and particle diffusion time

Table 1
Adjustable parameters of the discrete equilibrium model (Eq. (2)) for the biosorption of lead (value ± standard error)

Biosorbent	Discrete model			R^2	S_R^2 ($\times 10^{-4}$ mmol g^{-1})^2
	Q_{max} (mmol g^{-1})	pK_H	pK_M		
Gelidium	0.26 ± 0.01	3.92 ± 0.07	4.02 ± 0.06	0.921	4.3
Algal waste	0.20 ± 0.01	4.13 ± 0.08	3.85 ± 0.07	0.915	2.6
Composite material	0.096 ± 0.003	4.7 ± 0.1	4.6 ± 0.1	0.922	6.7

Table 2
Adjustable parameters of the continuous equilibrium model (Eq. (3)) for the biosorption of lead (value ± standard error)

Biosorbent	Continuous model					R^2	S_R^2 $(\text{mmol g}^{-1})^2$
	pK'_M	n_M	p	n_H/n_M	m_M		
Gelidium	3.8 ± 0.1	0.55 ± 0.03	1.0 ± 0.07	0.77	0.55	0.932	4.0×10^{-4}
Algal waste	3.7 ± 0.2	0.63 ± 0.05	0.85 ± 0.09	0.68	0.54	0.844	5.0×10^{-4}
Composite material	4.2 ± 0.1	0.68 ± 0.04	0.44 ± 0.03	1.1	0.30	0.941	5.3×10^{-5}

constant (τ_d), which depends on the intraparticle homogeneous diffusion coefficient.

A collocation on finite elements method was used to solve the non-linear parabolic PDE with the initial and boundary conditions for each model equation. It consists in representing the solution by a series expansion of degree N polynomials [14].

3.4.2. Linear driving force model (LDF)

If the average metal concentration inside the particle is used instead of a concentration profile, the following equations must be considered:

Kinetic law:

$$\frac{d\langle y(t)\rangle}{dt} = k_p a_p [y_M - \langle y(t)\rangle]; \qquad a_p = \frac{1}{L} \tag{14}$$

where k_p is the mass transfer coefficient for intraparticle diffusion (cm s^{-1}) and a_p is the specific surface area of the thin plates particles (cm^{-1}).

Equilibrium law:

$$y_M = \frac{K_L C_{b_0} y_b(t)}{1 + K_L C_{b_0} y_b(t)} \tag{15}$$

Mass conservation in the fluid inside the closed vessel:

$$\langle y(t)\rangle = \frac{1}{\xi}(1 - y_b(t)) \tag{16}$$

Initial condition:

$$t = 0: \quad y_b(t) = 1, \qquad \langle y(t)\rangle = 0 \tag{17}$$

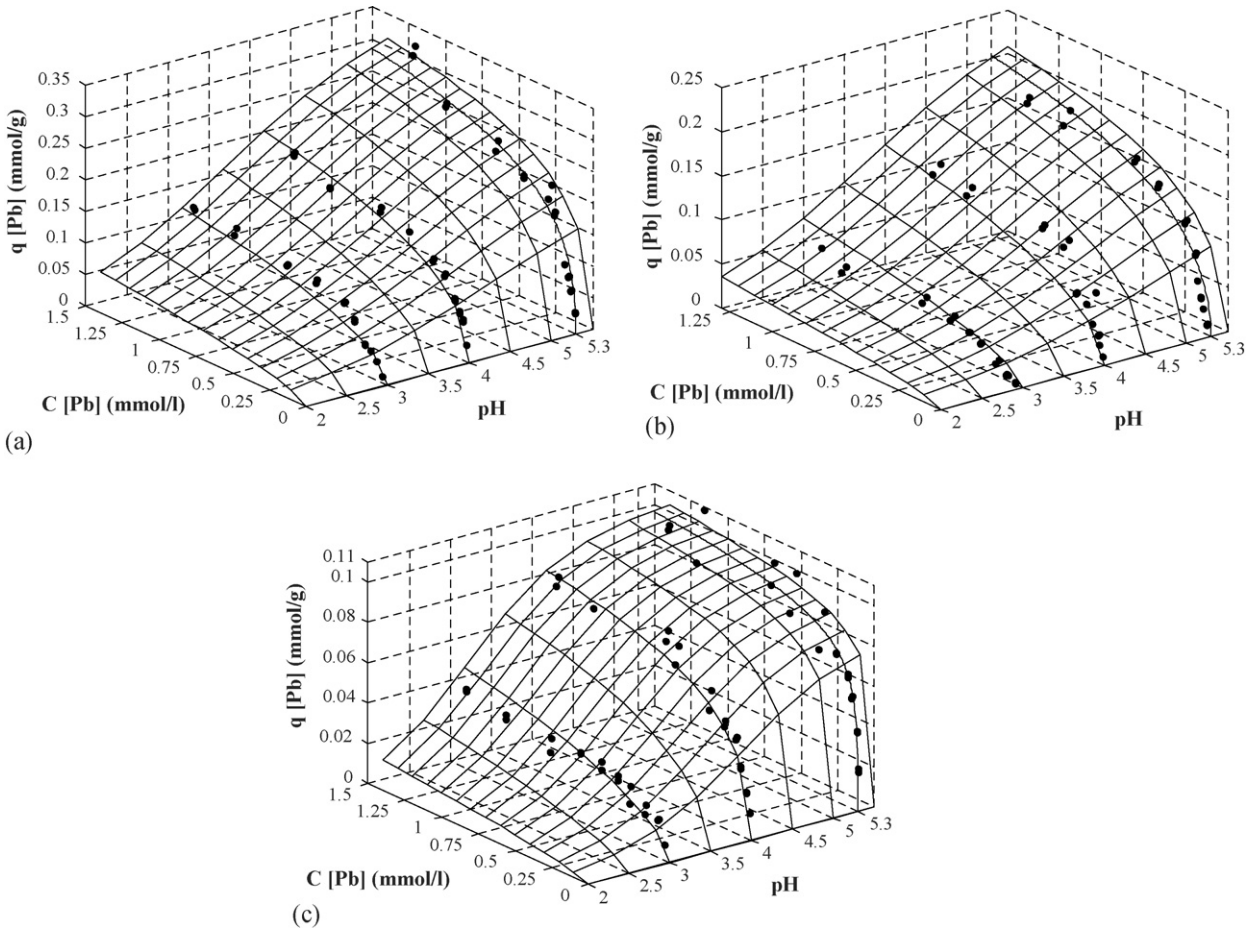

Fig. 2. Lead sorption isotherm surface: experimental data and continuous equilibrium model mesh. Solution pH 3, 4 and 5.3, lead concentration 0.0–1.5 mmol l^{-1}. Algae *Gelidium* (a), algal waste (b) and composite material (c).

Rearranging Eqs. (14)–(16), we obtain the following expression:

$$\frac{1}{k_p a_p}\frac{dy_b(t)}{dt} + \left(\frac{\xi K_L C_{b_0}}{1 + K_L C_{b_0} y_b(t)} + 1\right) y_b(t) = 1 \quad (18)$$

Eq. (18) can be solved analytically and the solution is given by

$$t = -\frac{1}{k_p a_p}\left\{\frac{1}{2c}\ln\left[\frac{y_b(t)^2 + a y_b(t) - c}{a - c + 1}\right] + \left(1 - \frac{a}{2c}\right)\left(\frac{1}{\alpha - \beta}\right)\ln\left[\frac{(1-\beta)(y_b - \alpha)}{(1-\alpha)(y_b - \beta)}\right]\right\} \quad (19)$$

where

$$a = \xi - 1 + \frac{1}{K_L C_{b_0}}; \qquad c = \frac{1}{K_L C_{b_0}};$$

$$\alpha = \frac{-a + \sqrt{a^2 + 4c}}{2}; \qquad \beta = \frac{-a - \sqrt{a^2 + 4c}}{2};$$

$$k_p a_p = \frac{D_h}{\phi L^2};$$

$$\phi = \frac{1}{3} \text{ (supposing a parabolic profile inside the particle)} \quad (20)$$

$$k_p a_p = \frac{3}{\tau_d} \text{ (mass transfer intraparticle resistance, min}^{-1}\text{)} \quad (21)$$

To predict metal concentration by using this model, the values of the following parameters are required: equilibrium isotherm parameters (q_{max}, K_L) at the solution pH, solution volume (V), initial Pb(II) concentration (C_{b_0}), biomass particles load (W) and particle diffusion coefficient (k_p).

3.5. Estimating model parameters

The experimental data obtained from equilibrium studies were fitted to the mathematical models by a non-linear regression method (FigSys for Windows from BIOSOFT). The model parameters were obtained by minimizing the sum of the squared deviations between experimental and predicted values. Model effectiveness was evaluated through the calculation of relative standard deviations (σ_i), sum of square residuals (S_R^2) and regression coefficients (R^2).

4. Results and discussion

4.1. Equilibrium studies

Equilibrium isotherms for lead biosorption on algae *Gelidium*, algal waste and composite material, at different pH, are presented in three-dimensional plots (Fig. 1(a–c)). The uptake capacity increases with the solution pH. The same result was obtained for copper removal by the same biosorbents [10] suggesting that competition for the active sites exists between the protons and metal ions. As Langmuir and Langmuir–Freundlich

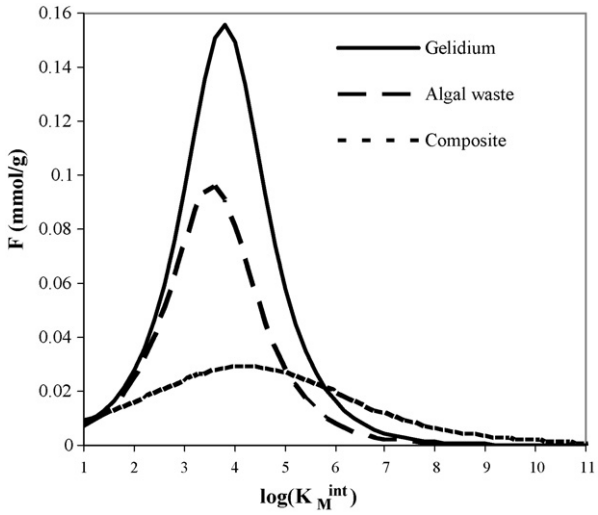

Fig. 3. Affinity distribution function for lead binding to carboxylic groups.

equations used to describe the equilibrium biosorption [11,12] do not include the influence of [H+], two equilibrium models have been developed to predict the influence of pH on biosorption. Carboxylic groups were considered to be the predominant

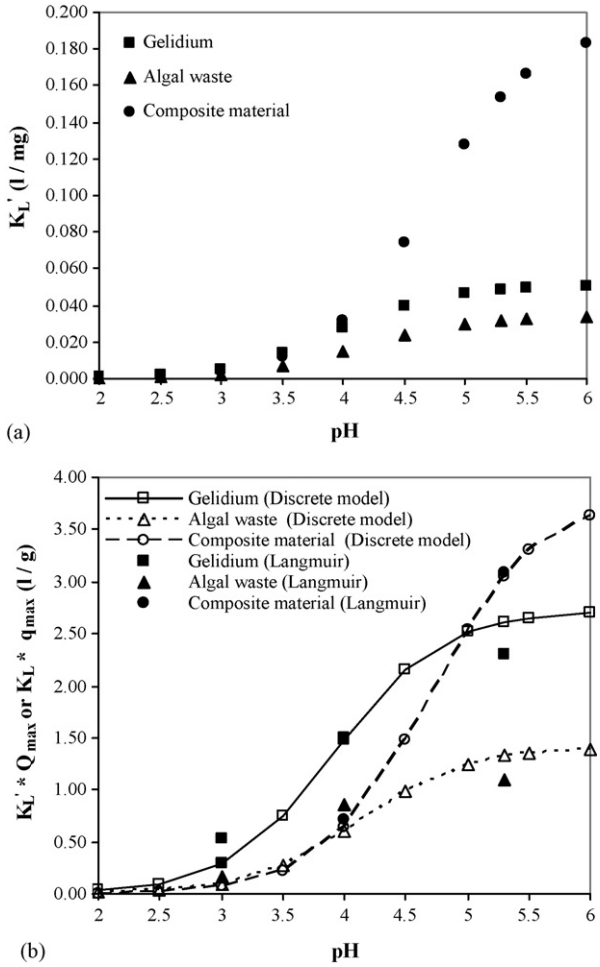

Fig. 4. Effect of pH on K'_L (a) and $K'_L Q_{max}$ (b) for algae *Gelidium*, algal waste and composite material.

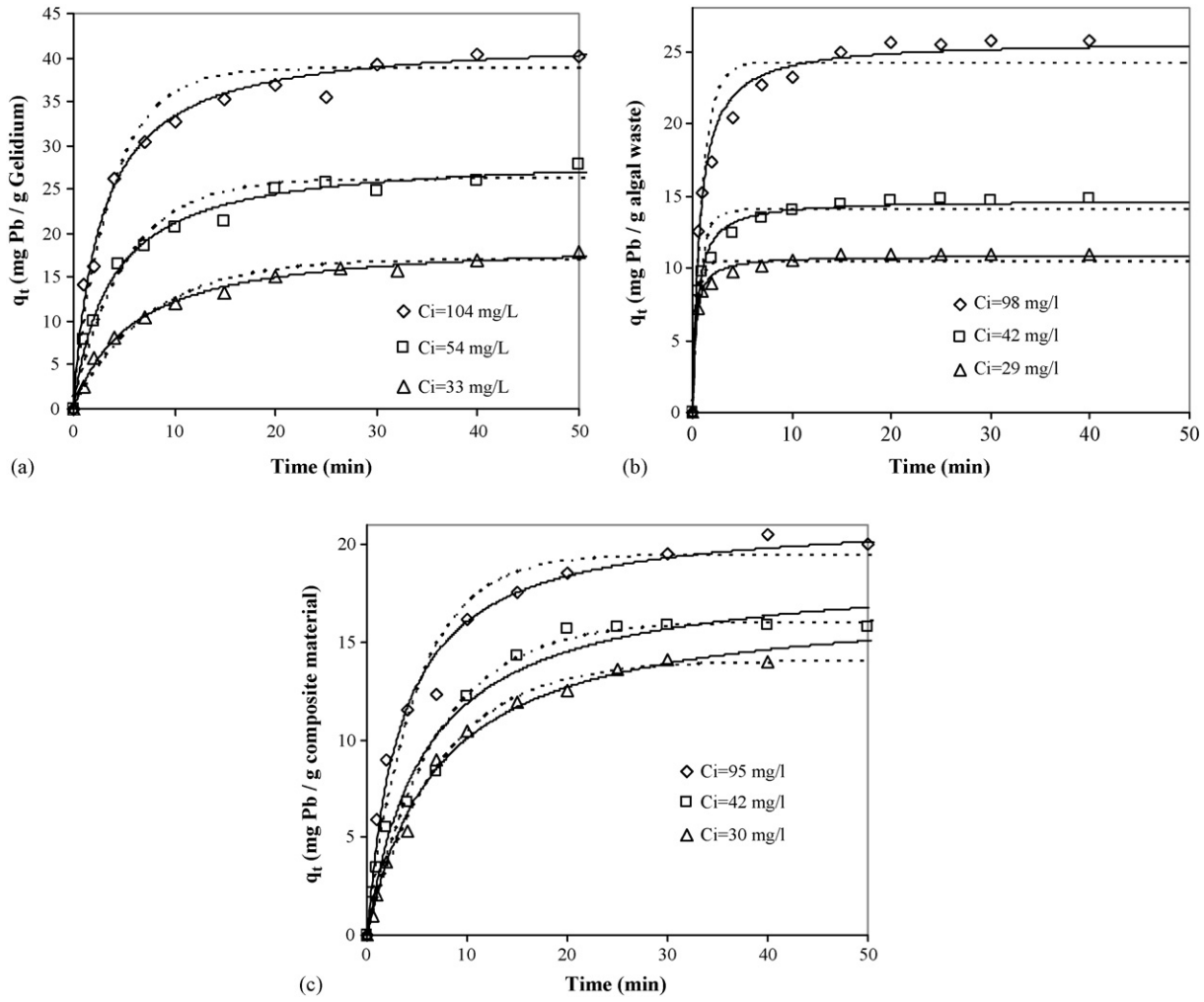

Fig. 5. Evolution of adsorbed Pb(II) concentration on Algae *Gelidium* (a), algal waste (b) and composite material (c), with contact time, for different lead initial concentrations. Experimental data and kinetic models: (- - -) pseudo-first-order Lagergren model and (—) pseudo-second-order model.

active sites to bind lead ions, because adsorption was studied at pH below 7 and, in this pH range, hydroxyl groups do not contribute to metal adsorption ($pK_H > 8.0$). The three adjustable parameters (Q_{max}, K_H and K_M), for the discrete biosorption model, are presented in Table 1. Similarly, the adjustable parameters considered for the continuous model (K'_M, n_M and p) are presented in Table 2. Other parameters were determined from potentiometric titrations ($Q_{max} = 0.36$, 0.23 and 0.16 mmol g^{-1}, $pK'_H = 5.0$, 5.3 and 4.4 and $m_H = 0.43$, 0.37 and 0.33, respectively, for algae *Gelidium*, algal waste and composite material) [10].

Experimental values are compared with the predicted ones in the Fig. 1(a–c) for the discrete model and in Fig. 2(a–c) for the continuous model, respectively, for algae *Gelidium*, algal waste

Table 3
Estimated parameters for the pseudo-first-order Lagergren model at different initial lead concentrations (value ± standard deviation)

Biosorbent	C_i (mg l^{-1})	Pseudo-first-order Lagergren model				
		q_M (mg g^{-1})	$k_{1,ads}$ (min^{-1})	R^2	S_R^2 (mg g^{-1})^2	r_{ads}(i) (mg g^{-1} min^{-1})
Gelidium	104	39 ± 1	0.26 ± 0.04	0.960	7.48	10.1
	54	26.1 ± 0.7	0.19 ± 0.02	0.962	3.55	5.0
	30	17.0 ± 0.4	0.13 ± 0.01	0.977	0.99	2.2
Algal waste	102	24.2 ± 0.8	0.93 ± 0.16	0.934	4.56	22.5
	42	14.0 ± 0.4	1.3 ± 0.2	0.937	1.33	18.2
	29	10.5 ± 0.2	1.9 ± 0.3	0.959	0.44	20
Composite material	95	19.5 ± 0.6	0.21 ± 0.03	0.963	2.19	4.1
	42	16.0 ± 0.5	0.15 ± 0.02	0.984	0.80	2.4
	30	14.0 ± 0.3	0.13 ± 0.01	0.996	0.13	1.8

Table 4
Estimated parameters for the pseudo-second-order model at different initial lead concentrations (value ± standard deviation)

Biosorbent	C_i (mg l^{-1})	Pseudo-second-order model				
		q_M (mg g^{-1})	$k_{2,ads}$ ($\times 10^2$ g mg^{-1} min^{-1})	R^2	S_R^2 (mg g^{-1})^2	r_{ads}(i) (mg g^{-1} min^{-1})
Gelidium	104	42.4 ± 0.7	0.87 ± 0.09	0.989	1.98	15.6
	54	30.0 ± 0.5	0.9 ± 0.1	0.989	0.94	8.1
	30	19.4 ± 0.3	0.88 ± 0.07	0.995	0.20	3.3
Algal waste	102	25.7 ± 0.5	5.4 ± 0.7	0.983	1.15	35.7
	42	14.7 ± 0.3	14 ± 2	0.984	0.32	30.3
	29	10.9 ± 0.1	31 ± 4	0.992	0.09	36.8
Composite material	95	21.5 ± 0.5	1.4 ± 0.2	0.985	0.73	6.5
	42	18.7 ± 0.8	0.9 ± 0.1	0.979	0.84	3.2
	30	17.2 ± 0.5	0.8 ± 0.1	0.995	0.17	2.4

Table 5
Percent of lead removal and *F*-test for residual variances of kinetic models

Biosorbent	C_i (mg l^{-1})	% removal	$n-1$	F_{cal}	$F_{1-\alpha}$	Statistically better
Gelidium	104	40	13:13	3.77	2.58	Second order
	54	52	13:13	3.78	2.58	Second order
	30	56	13:13	5.07	2.58	Second order
Algal waste	102	51	11:11	3.97	2.82	Second order
	42	70	11:11	4.13	2.82	Second order
	29	77	11:11	4.78	2.82	Second order
Composite material	95	21	11:11	3.01	2.82	Second order
	42	38	12:12	1.06	2.69	No difference
	30	47	11:11	1.36	2.82	No difference

and composite material. Both models can be used to predict the equilibrium sorption data at different pH and lead concentration.

The affinity distribution functions for lead adsorption on carboxylic groups shown in Fig. 3 were obtained by the Sips distribution with the parameters presented in Table 2. The function peaks correspond to the pK'_M values. The highest peak was obtained for algae *Gelidium*, because it has more carboxylic groups and consequently is the better biosorbent for lead. The width of the Sips distribution measured by p, gives indication about the active sites heterogeneity, changing between 1 for complete homogeneity and 0 for a highly heterogeneous biosorbent. Values of $p = 1.0$, 0.85 and 0.44 obtained, respectively, for algae, algal waste and the composite material, indicate a greater contribution of binding groups with low affinity for the composite material, then resulting in a wide distribution of affinities.

The ratio n_H/n_M is directly related to the exchange ratio between protons and metal ions (r_{ex}). r_{ex} can change over the range $0 < r_{ex} < n_H/n_M$, the greatest value being found for small p (high heterogeneity), low metal concentration and low pH. This is true when most of the sites are occupied by protons and the binding reaction approaches a "normal" ion exchange reaction. Under these conditions, the ratio n_H/n_M represents some kind of reaction stoichiometry [15]. In Table 2, n_H/n_M values for algae, algal waste and composite material indicate that for each millimoles of metal ion that is bonded 0.77, 0.68 and 1.1 mmol of protons are released, respectively. Similar values were determined for copper biosorption in the same biosorbents [10]. In the same way, desorption of Cu by protons is a reversible exchange with stoichiometric coefficients of 0.70, 0.73 and 0.76, respectively [10].

For the composite material, $n_M < n_H$, suggesting that there are some protonated sites with low affinity for lead ions or reflecting some degree of multi-dentism. Contrarily, for algae and algal waste, $n_M > n_H$, then the maximum binding of species i is greater than that for protons. This could reflect some degree of cooperativity [15].

The apparent equilibrium affinity (K_M) for lead, obtained by the discrete model, can be compared with the apparent affinity constant, K'_L, of Langmuir equation. Dividing Eq. (2) by $1 + K_H C_H$, gives:

$$q_M = \frac{Q_{max} K'_L C_M}{1 + K'_L C_M} \quad (22)$$

Table 6
Estimated kinetic constants using the pseudo-first-order Lagergren model (Eq. (24))

Biosorbent	$k_{1,ads}$		R^2	q_M		R^2
	a	*b*		*a*	*b*	
Gelidium	0.020	0.556	0.993	1.78	0.667	0.998
Algal waste	10.6	−0.533	0.930	1.18	0.655	0.997
Composite material	0.032	0.415	0.999	5.51	0.280	0.985

where

$$K'_L = \frac{K_M}{1 + K_H C_H} \quad (23)$$

K'_L is the apparent equilibrium affinity from Langmuir model ($1\,mg^{-1}$).

Values of K'_L decrease when decreasing pH from 5.3 to 4 (43, 54 and 79%, respectively, for algae, algal waste and composite material) (see Fig. 4(a)), due to competition of lead ions with protons for the active sites. At pH 5.3 higher K'_L values were found for lead adsorption on composite material. Lower affinity values were found for adsorption of copper ions on the same biosorbents [10].

Fig. 4(b) shows the pH influence on the product $Q_{max}\ K'_L$, which represents the initial slope of the Langmuir equation or the driving force for lead adsorption at low lead concentration. As pH increases the initial slope of the Langmuir equation increases. For pH < 5.3, algae is the better biosorbent, even at low lead concentration. For pH > 5.3, the results may be imprecise because equilibrium was not studied at pH values higher than 5.3.

Fig. 4(b) also shows the values of $q_{max}K_L$ for pH 3, 4 and 5.3, obtained from the parameters of the Langmuir equation (q_{max}—maximum uptake capacity; K_L—Langmuir constant affinity) presented in a previous work [11,12]. Those values are similar to those obtained from the parameters of the discrete model.

4.2. Kinetic studies

Fig. 5(a–c) illustrates the evolution of lead uptake with time for three different initial lead concentrations. Adsorption occurs mainly within the first 20, 10 and 30 min, respectively, for algae, algal waste and composite material. This difference is due to different intraparticle diffusion resistance. During the agar extraction process the porosity of the algal biomass increases, reducing the resistance to intraparticle diffusion. The active component (algal waste) present in the composite material is immobilized with PAN, adding another resistance to metal diffusion.

Faster kinetics has significant practical importance as it will facilitate the scale-up of the process to small reactor volumes, ensuring efficiency and economy. This behaviour is typical of biosorption of metals involving purely weak intermolecular forces between the biomass and the metal in solution (physical adsorption).

4.2.1. Kinetic models

Two kinetic models were applied to describe the biosorption kinetics of lead. Fig. 5(a–c) compares the kinetic data with the curves predicted by the pseudo-first-order Lagergren and pseudo-second-order models. Model parameters are presented in Tables 3 and 4. It can be seen that both models fit well the

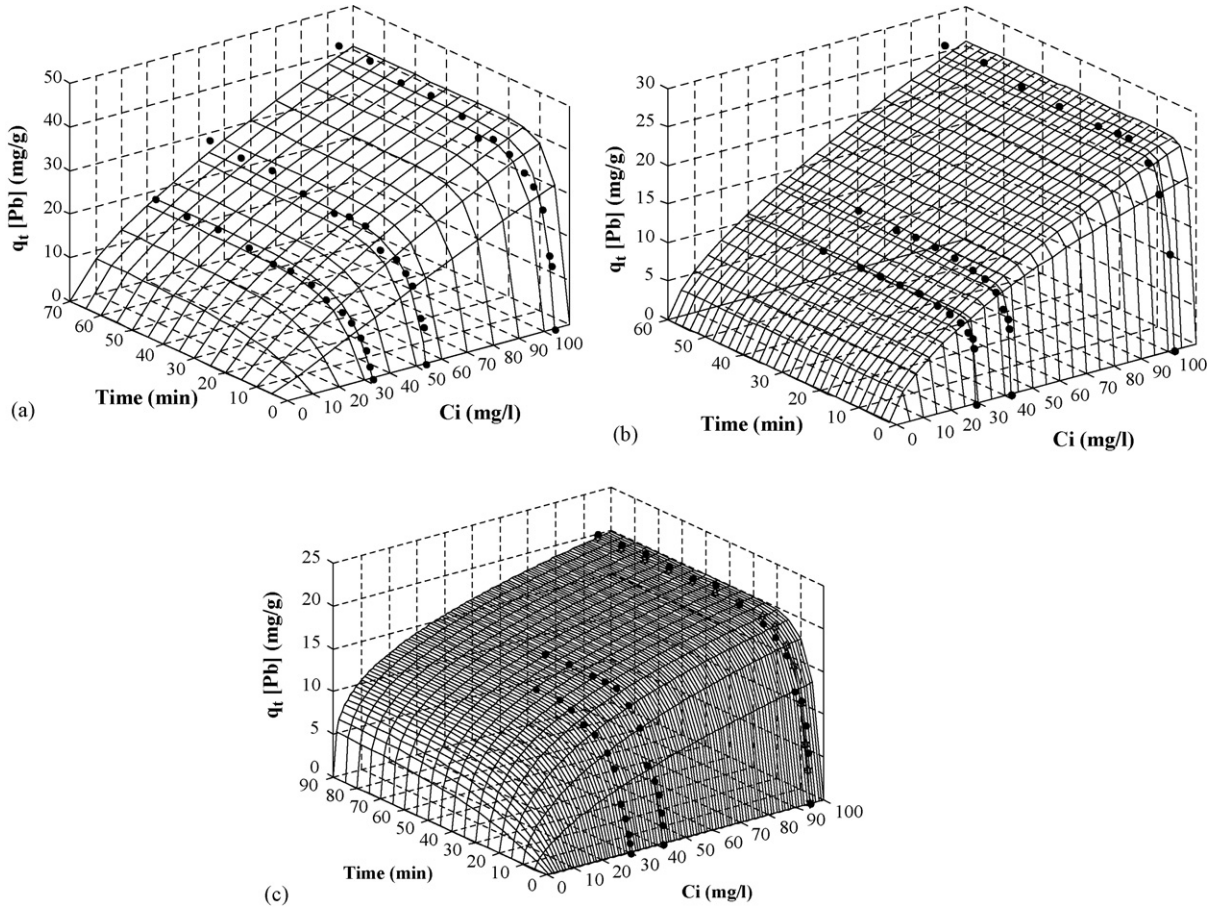

Fig. 6. Effect of initial Pb(II) concentration on biosorption at different contact times: (a) algae *Gelidium*; (b) algal waste; (c) composite material.

experimental data for the three initial lead concentrations. The performances of the two models were also compared by the *F*-test. Results in Table 5 show that the pseudo-second-order model is better for the algae *Gelidium* and algal waste. For the composite material, although the pseudo-second-order model is better for the higher lead concentration, no significant difference exists between the two models when considering the whole concentration range.

The initial concentration provides an important driving force to overcome all mass transfer resistance of Pb(II) between the aqueous and solid phases. A higher initial concentration of Pb(II), increases the initial biosorption rate (Tables 3 and 4) and the equilibrium uptake. For the algal waste these values are independent of the initial lead concentration, suggesting that the intraparticle diffusion is extremely fast.

The percentage of lead removal from solution increases as initial lead concentration decreases (Table 5), due to the existence of a constant number of active sites available for metal ions binding. A similar trend was also reported by other authors [16,17].

The kinetic parameters given by the pseudo-first-order Lagergren are correlated to the initial lead concentration by the following equation:

$$k_{1,\text{ads}} \text{ or } q_M = a\exp(bC_i) \quad (24)$$

where a and b are constants given in Table 6. Substituting the values of q_M and $k_{1,\text{ads}}$ from Eq. (24) into Eq. (4), the uptake capacity under different values of initial lead concentration and contact time can be predicted as shown by surfaces in Fig. 6(a–c). Increasing the initial metal concentration, the uptake capacity and biosorption rate also increase, and the saturation of the material is achieved in a short time. Lead uptake capacity decreases 56.4, 56.6 and 28.2% from the higher to the lower initial lead concentration. This kind of analysis can be useful for the process application, since the influence of the contact time and the initial concentration on the metal uptake capacity can be easily predicted.

4.2.2. Mass transfer models

In order to predict lead uptake as a function of contact time two mass transfer models were developed. Figs. 7 and 8 present the predicted curves by the two models, showing a good agreement with the experimental data for different initial concentra-

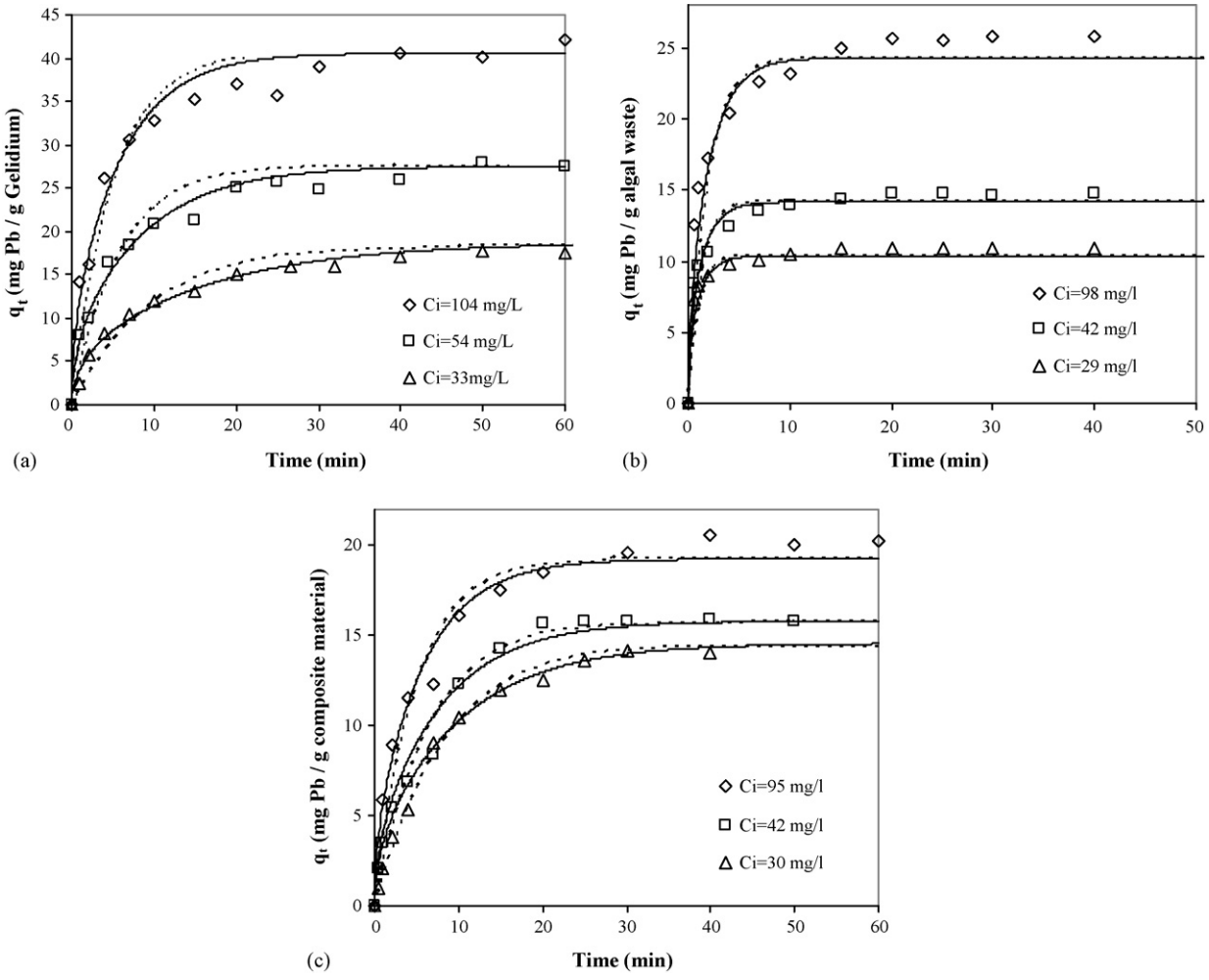

Fig. 7. Evolution of adsorbed Pb(II) concentration on Algae *Gelidium* (a), algal waste (b) and composite material (c), with contact time, for different values of the initial concentration: experimental data and mass transfer kinetic models. Homogeneous particle diffusion model (—) and linear driving force model (- - -).

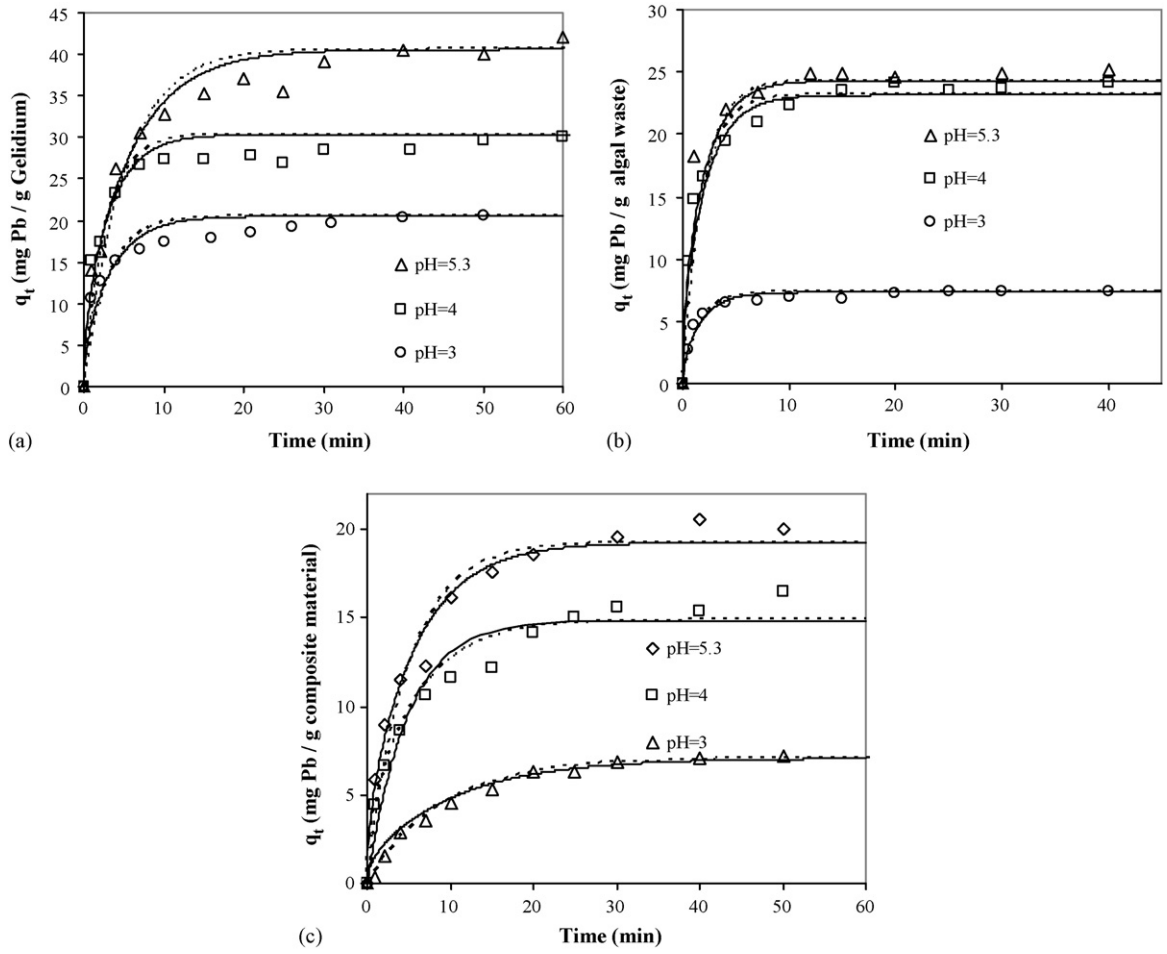

Fig. 8. Evolution of adsorbed Pb(II) concentration on Algae *Gelidium* (a), algal waste (b) and composite material (c), with contact time, for different values of pH: experimental data and mass transfer kinetic models. Homogeneous particle diffusion model (—) and linear driving force model (- - -).

tions and pH, respectively. In Table 7 are presented the time diffusion constants obtained for both models, which are very similar. Increasing the initial metal concentration, the time diffusion decreases, showing the importance of the concentration driving force to overcome the intraparticle diffusion resistance, since the film resistance is negligible for high stirring rate. Increasing solution pH, τ_d increases for algae and algal waste and decreases for the composite material. For low pH values,

Table 7
Estimated parameters for the linear driving force and homogeneous particle diffusion models

Biosorbent	C_i (mg l^{-1})	pH	LDF model		Homogeneous diffusion model		
			$k_p a_p$ (min^{-1})	τ_d (min)	τ_d (min)	D_h (cm^2 s^{-1})	D_h (average) ($\times 10^{-8}$ cm^2 s^{-1})
Gelidium	104	5.3	0.17	18	17.5	2.4×10^{-8}	
	106	4.0	0.33	9.1	9	4.6×10^{-8}	3.7
	106	3.0	0.30	10	10	4.2×10^{-8}	
	54	5.3	0.12	25	30	1.4×10^{-8}	3.4
	33	5.3	0.06	50	65	6.4×10^{-9}	
Algal waste	98	5.3	0.39	7.7	8	5.2×10^{-8}	
	112	4.0	0.45	6.7	7	6.0×10^{-8}	6.5
	106	3.0	0.6	5.0	5	8.3×10^{-8}	
	42	5.3	0.38	7.9	7	6.0×10^{-8}	5.7
	29	5.3	0.38	7.9	7	6.0×10^{-8}	
Composite material	95	5.3	0.25	12	13	3.2×10^{-8}	
	100	4.0	0.20	15	15	2.8×10^{-8}	2.5
	98	3.0	0.11	27.3	27	1.5×10^{-8}	
	42	5.3	0.15	20	21	2.0×10^{-8}	2.2
	30	5.3	0.10	30	29	1.4×10^{-8}	

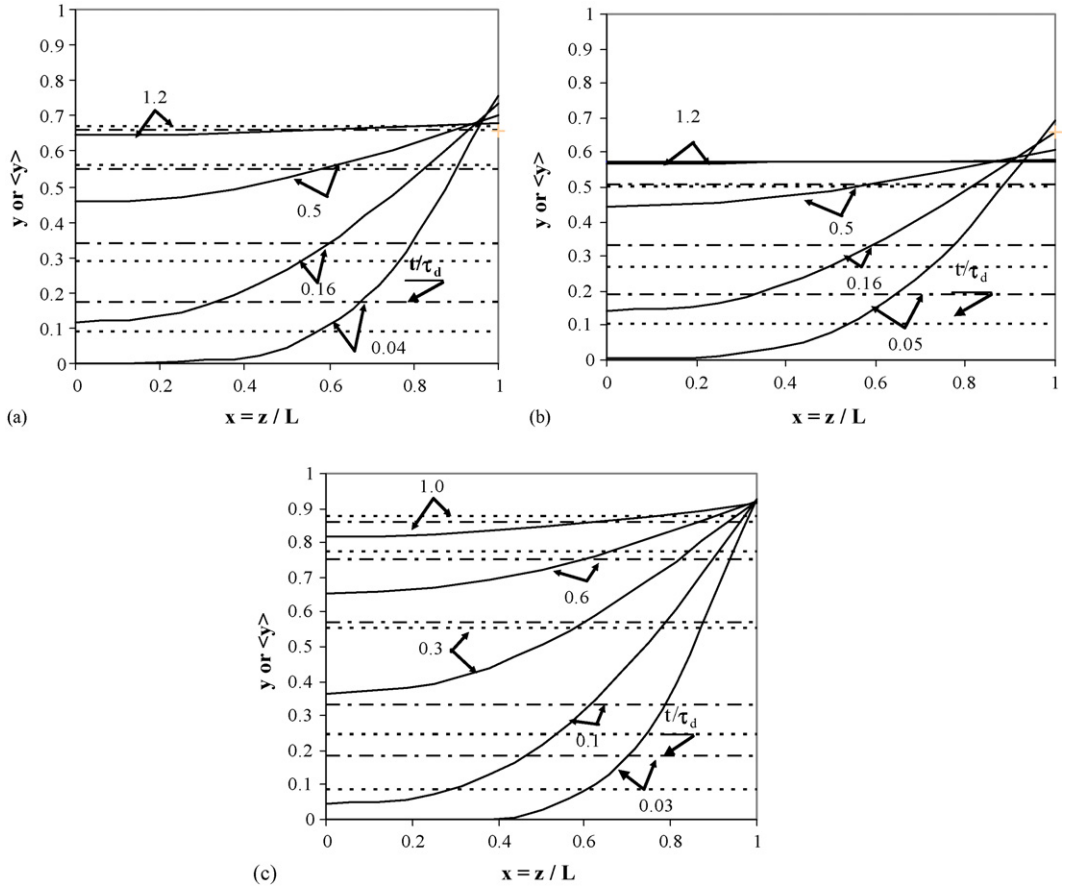

Fig. 9. Concentration profiles inside the particle for different values of t/τ_d. Pb(II) concentration predicted by the homogeneous particle diffusion model (—) and average metal concentration in the particle predicted by the linear driving force model (- - -) and homogeneous diffusion model (- - -): (a) algae *Gelidium*; (b) algal waste; (c) composite material, for $C_i \cong 100\,mg\,l^{-1}$; pH 5.3.

diffusion resistance increases due to the competition with protons for the binding sites. On the other hand, lead affinity for the binding sites decreases with pH (Fig. 4(a)), also due to the competition with protons. These two factors determine the diffusion rate resistance.

Values of the intraparticle homogeneous diffusion coefficients (D_h) for different initial concentrations and pH values, considering the thickness of the thin plate particles as 0.1 mm (determined by microscopic observations), are also presented in Table 7. Average diffusion coefficients for lead adsorption on each biosorbent are similar for different pH values and initial lead concentrations and are also very close to the obtained for Cu adsorption on the same biosorbents [10].

Concentration profiles inside the particle for different values of dimensionless time (t/τ_p) are presented in Fig. 9(a–c) for the initial lead concentration $\cong 100\,mg\,l^{-1}$. The metal concentration inside the particle follows approximately a parabolic profile for low values of (t/τ_p) and a linear profile near the equilibrium. The average metal concentrations inside the particle predicted by the two models are different initially, but as (t/τ_p) increases they become closer and equal at equilibrium. So, the assumption made in LDF model is well accomplished.

The biosorption rate for the pseudo-first-order model is defined as

$$r_{ads} = \frac{dq_t}{dt} = k_{1,ads}(q_M - q_t) \quad (25)$$

Integrating this equation, we get the kinetic pseudo-first-order Lagergren model. Eq. (25) is similar to the kinetic law used in LDF mass transfer model, where $k_p a_p = k_{1,ads}$. The respective values, are of the same magnitude, with the exception of the algal waste, where $k_{1,ads}$ is higher than $k_p a_p$.

5. Conclusions

Algae *Gelidium* biomass and the industrial algal waste from agar extraction are able to remove and accumulate Pb(II) from aqueous solutions at very low concentrations.

Biosorption of lead ions at different pH values is well described by discrete and continuous distributions of carboxylic sites. These models can predict lead uptake at different equilibrium lead concentrations and pH, giving a major advantage relatively to Langmuir equation.

Lead affinity for carboxylic sites given by the Sips distribution shows a narrow distribution for algae and algal waste, but it is wide for the composite material.

Kinetic experiments at different initial lead concentrations and pH values are well described by the pseudo-first- and

second-order models. Mass transfer models successful predict the lead uptake at different lead concentrations and pH values, showing a parabolic concentration profile inside the particles.

Acknowledgements

This work was developed under the project POCI/AMB/57616/2004. The authors are grateful to the Portuguese Foundation for Science and Technology (FCT) for the financial support and V. Vilar's doctorate scholarship.

References

[1] WHO, Environmental Health Criteria 165: Inorganic Lead, WHO, Geneva, 1995.
[2] Y.S. Ho, C.T. Huang, H.W. Huang, Equilibrium sorption isotherm for metal ions on tree fern, Proc. Biochem. 37 (2002) 1421–1430.
[3] C. Alexandra, C. Plette, M.F. Benedectti, W.H.V. Riemsdijk, Competitive binding of protons, calcium, lead, and zinc to isolated cell walls of a gram-positive soil bacterium, Environ. Sci. Technol. 30 (1996) 1902–1910.
[4] P.A. Marques, H.M. Pinheiro, J.A. Teixeira, M.F. Rosa, Removal efficiency of Cu^{2+}, Cd^{2+} and Pb^{2+} by waste brewery biomass: pH and cation association effects, Desalination 124 (1999) 137–144.
[5] Y.S. Ho, G. McKay, Batch sorber design using equilibrium and contact time data for the removal of lead, Water Air Soil Pollut. 124 (2000) 141–153.
[6] Z.R. Holan, B. Volesky, Biosorption of lead and nickel by biomass of marine algae, Biotechnol. Bioeng. (1994) 1001–1009.
[7] O. Raize, Y. Argaman, S. Yannai, Mechanisms of biosorption of different heavy metals by brown marine macroalgae, Biotechnol. Bioeng. 87 (2004) 451–458.
[8] S. Klimmek, A. Wilke, G. Bunke, R. Buchholz, H.J. Stan, Comparative analysis of the biosorption of cadmium, lead, nickel, and zinc by algae, Environ. Sci. Technol. 35 (2001) 4283–4288.
[9] S. Schiewer, Modelling complexation and electrostatic attraction in heavy metal biosorption by *Sargassum* biomass, J. Appl. Phycol. 11 (1999) 79–87.
[10] V.J.P. Vilar, Remoção de iões metálicos em solução aquosa por resíduos da indústria de extracção do agar, Ph.D. Thesis, Faculdade de Engenharia da Universidade do Porto, Porto, 2006.
[11] V.J.P. Vilar, C.M.S. Botelho, R.A.R. Boaventura, Influence of pH, ionic strength and temperature on lead biosorption by *Gelidium* and agar extraction algal waste, Proc. Biochem. 40 (2005) 3267–3275.
[12] V.J.P. Vilar, F. Sebesta, C.M.S. Botelho, R.A.R. Boaventura, Equilibrium and kinetic modelling of Pb^{2+} biosorption by granulated agar extraction algal waste, Proc. Biochem. 40 (2005) 3276–3284.
[13] V.J.P. Vilar, C.M.S. Botelho, R.A.R. Boaventura, Equilibrium and kinetic modelling of Cd(II) biosorption by algae *Gelidium* and agar extraction algal waste, Water Res. 40 (2006) 291–302.
[14] N. Madsen, R. Sincovec, Pdecol: general collocation software for partial differential equations, ACM Trans. Math. Software 5 (1979) 326–351.
[15] D.G. Kinniburgh, W.H.V. Riemsdijk, L.K. Koopal, M. Borkovec, M.F. Benedetti, M.J. Avena, Ion binding to natural organic matter: competition, heterogeneity, stoichiometry and thermodynamic consistency, Colloids Surf. A 151 (1999) 147–166.
[16] B. Benguella, H. Benaissa, Cadmium removal from aqueous solutions by chitin: kinetic and equilibrium studies, Water Res. 36 (2002) 2463–2474.
[17] A. Agrawal, K.K. Sahu, B.D. Pandey, Removal of zinc from aqueous solutions using sea nodule residue, Colloids Surf. A 237 (2004) 133–140.